

1 **Recycling of waste coal dust for the energy-efficient fabrication of**
2 **bricks: A laboratory to industrial-scale study**
3

4 Milica Vidak Vasić^{a,*}, Gaurav Goel^{b,c}, Miloš Vasić^a, Zagorka Radojević^a
5

6 ^a*Institute for Testing of Materials IMS, Bulevar vojvode Mišića 43, 11000 Belgrade,*
7 *Serbia*

8 ^b*School of Engineering, London South Bank University, 103 Borough Road, London,*
9 *SE10AA, UK*

10 ^c*School of Aerospace, Transport and Manufacturing, Cranfield University, MK430AL,*
11 *UK*

12
13 *Corresponding author. *E-mail address:* milica.vasic@institutims.rs (M. V. Vasić)
14

15 **Abstract**

16 In this study, an optimal mixture of loess brick clays and waste coal dust in
17 laboratory hollow blocks production is determined with the aim of promoting
18 sustainable development in terms of saving resources and energy. The novelty of the
19 work lies in the first-time utilization of waste coal dust in combination with loess soil
20 brick-making thus bolstering European effort on waste utilization. The mentioned is
21 also in line with UN sustainable development goals, SDG 12 and 9. The chemical and
22 mineralogical contents of the clays were obtained using various chemical
23 characterization methods, and thermal behavior by using dilatometry and
24 simultaneous DSC/TG analysis. The important ceramic and technological
25 characteristics of the extruded brick clay and waste coal dust composite samples
26 during molding, drying, and firing were obtained. The chosen mixture of 70 %
27 calcareous clay and 30 % plastic clay to 3 % of high-calorie waste coal dust is found
28 optimal. Industrial-scale optimal blocks (250x190x190 mm³) with 60 % of vertical voids
29 were fired in a tunnel kiln, and the firing regime was recorded. It is determined that the
30 regime must be corrected in the firing and cooling zone since the differences
31 measured by thermo-couples were up to 180 °C. The industrial prototype was found
32 to be of satisfactory quality meeting the requirements of water absorption and
33 compressive strength as per European and other international standards. The study
34 was first of a kind detailed characterization of the industrial size bricks encompassing

35 waste coal dust and loess brick clays, with the emphasis on the usability in the
36 industry, and additionally recording and correcting of the firing regime in a tunnel kiln.
37 The product is recyclable and can be disposed of safely after the end of life.

38

39 *Key words:* Loess brick clay; Coal dust; Optimal mixture; Tunnel kiln; Firing regime;
40 Optimization

41

42 **1. Introduction**

43

44 Thermal power plants are considered the main sectors in the economy of
45 Serbia. In terms of the annual production of lignite, Serbia ranks 10th in the world. The
46 estimated reserves of this coal are 10 % of the total in Europe. About 40 million tons
47 of lignite are extracted daily in the country for electric power generation. Although it is
48 the greatest treasure in the region, lignite could prove to be the most prominent
49 problem. Being low-caloric and with huge moisture content, lignite is the worst quality
50 coal - it has low thermal power, leaves a lot of ash when burned, and leads to
51 increased gas emissions (such as CO₂ and SO₂). Many studies presented the
52 possibility of using fly and landfill ashes in different applications, but only 3 % of total
53 ashes are spent in the cement industry in Serbia, while the brick industry avoids using
54 it (Arsenović et al., 2015a; Gupta, 2017; Vukićević et al., 2018). Besides, there is no
55 published research on using coal washery rejects such as waste coal dust in the
56 country, and it is not even considered a valuable waste (Vijayan and D. Parthiban,
57 2020).

58 Throughout coal mining and washing, the waste remains in up to 15 % (Haibin
59 and Zhenling, 2010). The coal is washed to improve its quality, in which process large
60 amounts of water are used, and the leftover material containing impurities is discarded.
61 Since the demand for coal as fuel is huge, a significant quantity of waste is generated
62 during mining and handling activities. The generated waste is among the prominent
63 environmental problems. Fortunately, the washery rejects are used in many sectors
64 such as the construction industry, as underground backfill material, or reused as
65 energy-containing matter (Fan et al., 2014; Li and Wang, 2019), etc. The studies
66 concerning the usage of coal production reject in the ceramic industry are scarce. Coal
67 mine waste rocks and treated coal mine tailings, containing soil and leftover coal dust,
68 were used to produce 50 % or 100 % eco-friendly bricks (Abi et al., 2011; Lemeshev

69 et al., 2004; Taha et al., 2016). It is shown that coal mining and processing waste can
70 be successfully used in wall tiles production in quantities up to 80 % (Stolboushkin et
71 al., 2016). Only two studies in literature used waste coal dust in brick making. The first
72 one showed that waste coal dust can be optimally added in a quantity of 10 wt % to
73 produce hand-molded bricks fired at 1000 °C with increased compressive strength and
74 reduced water absorption compared to the pure clay bricks (Gökçe et al., 2018), but
75 the more detailed research is needed. The other work reported that the addition of dry
76 waste coal dust in a quantity of 3 % and 6 % in plastic clay is optimal for the production
77 of hollow blocks (Arsenović et al., 2015b), yet there is the need for testing the
78 possibility of using loess soil as the base material.

79 Loess soils are not amongst the highest quality raw materials in the brick
80 industry, and, as such, are rarely studied. They are characteristic for high contents of
81 carbonates and alevrolite-sized fraction, but also a sequence of the buried soil rich in
82 clay minerals. This material can be generally used in the production of bricks without
83 cavities but also can be enriched to produce modern energy-efficient hollow blocks
84 (Arsenović et al, 2014; Vasić et al., 2020). The important fact is that the deposits
85 consist of a lesser quantity of the buried soil (high contents of clay minerals and lack
86 of carbonates) in comparison to the calcareous clay.

87 The possibility of mixing waste into the soil to produce bricks has been
88 frequently explored during the last decades at a global level. The studies intend to
89 manufacture bricks with the improved porosity, and thus lowered thermal conductivity,
90 bearing in mind the possibly increased carbon footprint. Besides, the savings in energy
91 and natural raw material are not to underestimate. Decreasing the plasticity of the mix
92 and possible uncontrolled release of energy throughout the firing are the main
93 concerns when designing the proper mixtures with different components (Arsenović et
94 al, 2015a; Bocanegra, 2019; Goel et al., 2018).

95 In this study, the composites of dry waste coal dust and loess brick clay are for
96 the first time analyzed in detail, and the mixture is optimized. It is hypothesized that
97 the addition of waste coal dust would improve the energy-efficiency of loess clay bricks
98 while firing at the same peak temperature and that the developed industrial products
99 will satisfy the corresponding EN norms. Besides, this study presents scaling up to the
100 production in the factory and correction of the firing regime in a tunnel kiln. It is
101 concluded that waste coal dust of 7.6 MJ/kg calorific value can be safely added in a

102 quantity of 3 % to loess calcareous clay, thus obtaining a 60 % of voids industrial
103 thermo-block.

104

105 **2. Materials and methods**

106

107 This section is focused on the characterization of the constituent materials and
108 reports on the scheme to obtain different mixes. Drying, moulding, and firing methods
109 are elaborated in detail. Finally, the procedure to obtain an industrial scale specimen
110 is described.

111

112 *2.1. Characterization and preparation of the raw materials and mixtures*

113

114 In this study, 2 primary loess brick clays (BC1 and BC2) from Vojvodina,
115 Serbia were used to make mixtures with waste coal dust as an eco-friendly raw
116 material in the brick industry. The clays (BC1 and BC2) were mixed in different
117 proportions to make 2 additional clays (BC3 and BC4). The coal dust, from the washing
118 process of coal, is taken off the filters from a coal washery. Two types of dust were
119 used: one of a higher calorific value and lower moist (CD1), and the other of lower
120 calorific value and higher moist content (CD2). The appearance of the as-received
121 samples of waste coal dust can be seen in Fig. 1, where All percentages refer to the
122 dry weight of both raw materials - brick clays and waste coal dust samples.

123



124

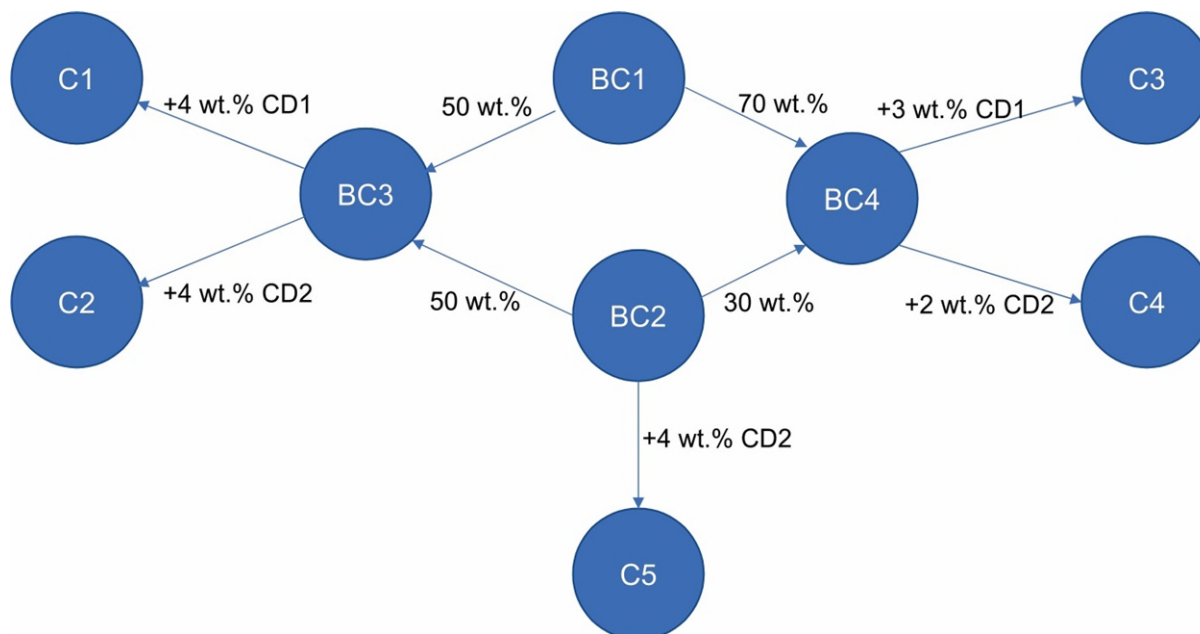
125

Fig. 1. The appearance of coal dust: (a) CD1, and (b) CD2.

126

127 The used experimental design is schematically presented in Fig. 2. It seems
 128 that the waste coal dust samples were similar besides the particle sizes, both
 129 containing coarse and small white grains.

130



131

132 **Fig. 2.** Schematic representation of the tested brick clays (BC) and waste coal dust
 133 (CD) mixtures to obtain C1-C5 composite materials.

134

135 The particle size distribution of the primary clay and dust materials is
 136 determined on as-received samples, while the mixtures containing waste coal dust
 137 were tested for granulometry after the grinding of CD1 and CD2 to fractions below 1
 138 mm. The method used for testing was a combination of hydrometry (for particles below
 139 0.063 mm) and wet sieve analysis according to the procedure described in the
 140 standard (SRPS U.B1.018). The samples pre-dried at 105 °C were sieved through the
 141 standard sieves, and the remains on each sieve were measured with an accuracy of
 142 0.1 wt.%. The solution of sodium hexametaphosphate was used as a dispersing agent
 143 (anticoagulant) of the fine-grained particles. The particle size ranges for the indicated
 144 particle sizes classes were clay (< 0.002 mm), alevrolite (0.002 mm – 0.06 mm), and
 145 sand (0.06 mm – 2 mm) (Kovács et al., 2006).

146 The primary samples of brick clays (BC1 and BC2) were dried in an oven at
 147 105 °C to a constant mass and subsequently dry-ground in a mill with a gap of 3 mm.
 148 The chemical and mineralogical compositions of the clays BC1 and BC2 is determined
 149 using the energy dispersive X-ray fluorescence (XRF) technique (Spectro Xepos; 50

150 W / 60 kV X-ray tube) and X-ray diffraction (XRD) analysis (Philips 1050; Ni-filtered
151 $\text{CuK}\alpha$ radiation of $\lambda = 1.5418$ nm and Bragg–Brentano focusing geometry, $6 - 90^\circ 2\theta$
152 range with the step of 0.05° , the exposure time was 6 s per step). The waste coal dust
153 samples (CD1 and CD2) were also dry-ground and the fraction passing the 1 mm sieve
154 is used in the mixtures. The macro and microelements contents in coal dust ash are
155 determined by XRF analyses.

156 The raw materials and mixtures were tested for thermal behavior using
157 differential scanning calorimetry and thermal gravimetry (SDT Q600, TA Instruments;
158 the flow of air $100 \text{ cm}^3/\text{min}$, the heating rate $20^\circ\text{C}/\text{min}$ up to 1000°C) and dilatometry
159 (Seteram instrument; the air atmosphere with a $20 \text{ ml}/\text{min}$ flow, the heating speed 20
160 $^\circ\text{C}/\text{min}$, the soaking time 1h).

161

162 *2.2. Molding and drying behavior of the laboratory samples*

163

164 After the initial preparation of the raw materials, the dry mixtures were made
165 following the experimental design defined in Fig. 2. Then, the materials were
166 moistened and left to rest for 24 h in sealed nylon bags for moisture homogenization.
167 Before molding, the moist samples were passed through a pair of rollers with a 0.5
168 mm gap for further homogenization of the moisture, but also the particle sizes. The
169 extrusion process is done under a vacuum in a laboratory Handle machine. The
170 samples in the form of $120 \times 50 \times 14 \text{ mm}^3$ tiles, $55.3 \times 36 \times 36 \text{ mm}^3$ hollow blocks, and
171 $30 \times 30 \times 30 \text{ mm}^3$ cubes were produced. The tiles mimicked roofing tiles, the cubes were
172 representative of a common brick without voids, and hollow blocks were of proportional
173 measures to industrial products containing about 50 % of voids. Afterward, the
174 samples were gently dried until 105°C to finally obtain the constant mass requirement.

175 The wet samples were used to test the sensitivity to drying by Bigot and
176 plasticity coefficient according to the method by Pfefferkorn (Arsenović et al, 2014).
177 The green (dry) samples were used to determine the remainings on the sieve (RS) of
178 0.063 mm by the wet procedure and the amount of total calcium and magnesium
179 carbonates (CCC) by a volumetric method (Scheibler's calcimeter) (Arsenović et al,
180 2014). CCC was also determined in the samples of coal dust.

181 Shaping moisture (SM) was determined in all kinds of molded samples and the
182 average value is presented, while drying shrinkage (DS) is measured using the tiles.
183 The parameters are determined as a percentage difference between wet and dry

184 samples in mass and length. The accuracy of the scale and caliper were to the second
185 decimal place.

186 The flattened laboratory samples having parallel sides were tested on an Alfred
187 Amsler hydraulic machine by which the compressive strength of the hollow blocks
188 (CSBD) and cubes (CSCD) is determined as an average value of the 3 samples. It is
189 taken care that the measured force is the one needed for the complete crash of the
190 samples, as required by the standard (SRPS EN 772-1).

191

192 *2.3. The firing of laboratory samples*

193

194 The firing was conducted in an electric laboratory oven in oxidizing conditions.
195 The chosen firing temperatures were 950 °C, 1000 °C, and 1050 °C. The slow-firing
196 regime is followed, and the soaking time was 2 h (Vasić et al., 2018). The cooling was
197 performed in natural conditions in a closed furnace.

198 The samples were measured for determination of loss on ignition (LOI) and
199 firing shrinkage (FS) immediately after the removal from the furnace. The weight
200 measurement was conducted on a scale with a precision of 0.01 g, while the caliper
201 used had 0.01 mm accuracy.

202 Bulk density (BD) and water absorption (WA) were determined in the standard-
203 defined ways (SRPS EN 772-13, SRPS EN 772-21).

204 The compressive strength of the laboratory fired hollow blocks (CSB) and cubes
205 (CSC) is determined as described in *Section 2.2*.

206

207 *2.4. Industrial probe*

208

209 After defining the optimal mixtures of the loess clays and two waste coal dust
210 samples, the industrial probe is done. The raw materials are mixed and a mound is
211 made to homogenize the material and the moisture. The primary processing involved
212 grinding below 1 mm. Larger concretions of carbonates (> 1 mm) require a special
213 processing line in the industry, with purifier and grinding in several stages so that they
214 do not remain in the form of CaO after firing. Due to hydration during the transition of
215 CaO to Ca(OH)₂, there is an increase in volume, and then by binding CO₂ from the air,
216 CaCO₃ is formed, which reaches about three times the volume of the initial CaO.
217 These reactions cause frequent "popping" and even damage to the product. The

218 blocks with about 60 % of vertical voids (250x190x190mm³) are made by the extrusion
219 process and tested for shaping moisture, plasticity coefficient, sensitivity to drying, and
220 remains on the 0.063 mm sieve (the methods explained in *Section 2.2*).

221 A multi-channel acquisition system THERM 3256-6 (Ahborn Mes und
222 Regelungstechnik), and 8 flexible NiCr-Ni thermocouples (type K), manufactured by
223 OMEGA, were used in the tunnel kiln firing regime diagnostic process. Thermo-
224 couples are placed in the lower, middle, and upper rows of the middle of the stack
225 from below through the wagon.

226 The compressive strength of the industrial probes is determined after flattening
227 the blocks` surfaces using mortar (SRPS EN 772-1), in the hydraulic press
228 Tonindustrie, Germany with a maximum force of 2000 kN. Water absorption is
229 measured according to SRPS EN 772-21:2012. Pre-dried samples are immersed in
230 cold water for 24 ± 0.5 h. The mass of the dry and soaked samples is measured with
231 an accuracy of 0.1 %. The results of water absorption are presented relative to the
232 mass of the dry sample.

233

234 **3. Results and discussion**

235

236 Properties of the lab- and industrial-scale bricks are determined in this section
237 and results are reported. The quality of these products is then determined and found
238 satisfactory meeting European norms.

239

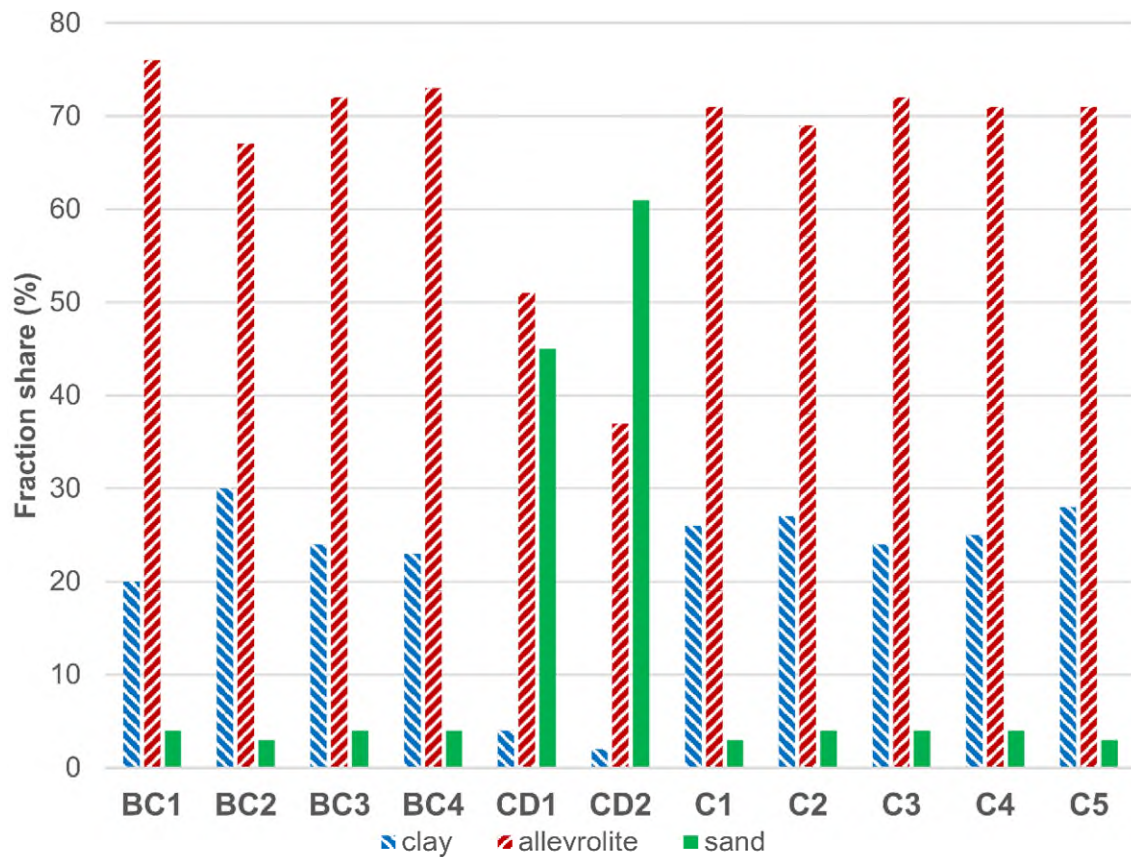
240 *3.1. Characteristics of the raw materials*

241

242 The macro-oxides composition of the primary brick clays, as determined by
243 XRF, is shown in Table 1. The main difference between the primary clays was the
244 carbonates: the sample BC1 contained high concentration and belonged to calcareous
245 clays (Taalab et al., 2019), while the sample BC2 showed a relatively low content of
246 calcite and magnesite. Besides, the clay BC1 contained more of a silt fraction and
247 belonged to silty loam (Fig. 3), while BC2 was a member of silty clay loam. It is
248 concluded (Fig. 3) that all the mixtures prepared were of similar granulometry as
249 primary raw materials (BC1 and BC2). The mixtures of the primary loess clays (BC3
250 and BC4) fell into a group of silty loam. Based on the results of these laboratory tests,
251 it can be concluded that the brick clay raw materials belonged to silty sediments

252 contaminated with carbonates. Carbonates are found in the raw material mainly in
 253 finely dispersed form, with a rare appearance of limestone concretions.

254



255

256 **Fig. 3.** Granulometry analysis of the samples prepared for molding.

257

258 The basic difference between the waste coal dust samples was in calorific
 259 values and moisture contents, as seen in Table 2. CD1 and CD2 showed
 260 approximately half the calorific value of lignite coal (Özdemir and Sarici, 2020). The
 261 XRF analysis of dried CD1 and CD2 is shown in Table 3. The content of ash was
 262 relatively high (Chen et al., 2015; Lingam et al., 2016), and the waste samples mostly
 263 contained SiO₂, Al₂O₃, Fe₂O₃, and CaO. Considering the microelements contents, and
 264 the EPA regulations, this waste is not hazardous, nor it can leach out from the final
 265 brick product.

266 **Table 1**

267 Chemical composition of the brick clays.

	SiO ₂	Al ₂ O ₃	Fe ₂ O ₃	CaO	MgO	Na ₂ O	K ₂ O	SO ₃	P ₂ O ₅	MnO	TiO ₂	LOI
	(%)	(%)	(%)	(%)	(%)	(%)	(%)	(%)	(%)	(%)	(%)	(%)
BC1	50.69	12.54	3.95	9.34	5.89	1.49	1.44	0.03	0.18	0.09	0.66	13.72
BC2	62.25	15.26	4.70	1.21	3.47	1.53	2.26	0.03	0.12	0.12	0.76	8.37

268

269 **Table 2**

270 Important characteristics of the waste coal dust samples.

	Clay- sized fraction (%)	Alevrolite- sized fraction (%)	Sand- sized fraction (%)	Content of moisture (%)	LOI (%)	Total contents of carbonates (%)	Ash content (%)	Calorific value (kJ/kg)	Maximum dry addition (%)
CD1	4	51	45	50.7	34.5	0.0	14.8	7569	4.62
CD2	2	37	61	56.3	29.5	0.0	14.2	6188	5.66

271

272

Table 3

273

XRF analyses of coal dust.

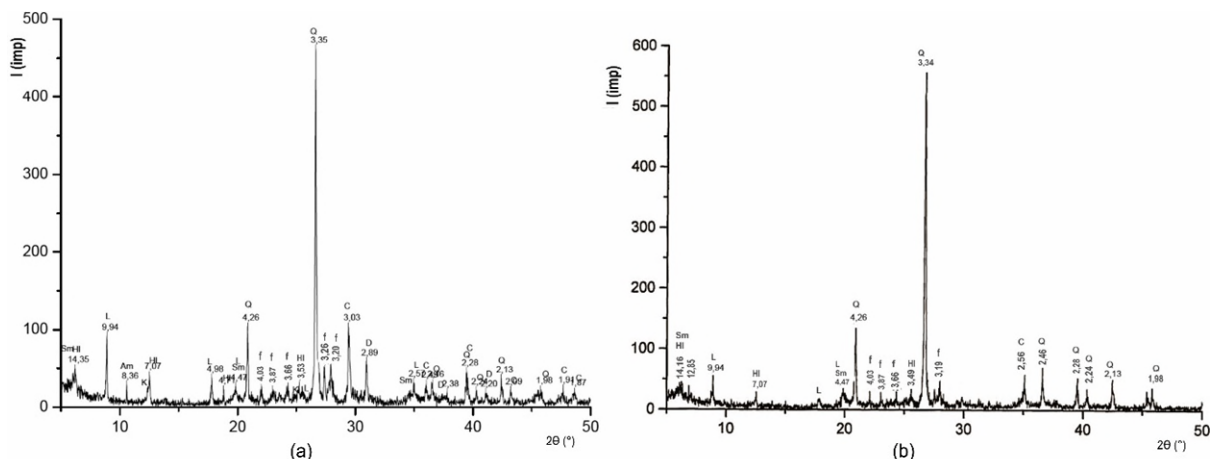
Sample	CD1	CD2
LOI (%)	76.77	64.04
SiO ₂ (%)	13.67	21.10
Al ₂ O ₃ (%)	4.36	7.72
Fe ₂ O ₃ (%)	1.61	2.04
CaO (%)	2.09	2.41
MgO (%)	0.78	1.06
Na ₂ O (%)	0.19	0.29
K ₂ O (%)	0.33	0.65
SO ₃ (%)	0.03	0.33
P ₂ O ₅ (%)	0.02	0.04
MnO (%)	0.03	0.04
TiO ₂ (%)	0.18	0.31
Ni, mg/kg	4.97	65.81
Co, mg/kg	0.98	16.90
Cu, mg/kg	1.81	37.40
Zn, mg/kg	9.04	11.76
As, mg/kg	0.30	32.44
Sr, mg/kg	53.20	70.84
Mo, mg/kg	0.67	2.59
Ba, mg/kg	8.83	222.95
Pb, mg/kg	0.28	<0.3
Sn, mg/kg	<0.3	<0.3
Bi, mg/kg	0.35	0.40
Hg, mg/kg	<0.2	0.07
Cd, mg/kg	<0.2	<0.2

274

275 The literature data show that the energy required for firing bricks ranges up
 276 to about 600 KJ/kg (Ferrer et al., 2015; Rimpel, 2019, Soussi et al., 2017). To roughly
 277 determine the maximum amounts of dry waste coal dust (CD1 and CD2) that could be
 278 added in the production of clay bricks, it is assumed that the amount required to
 279 compensate all the necessary energy is 350 KJ per kg of goods. The results presented
 280 in Table 2 show that the contents of dust must not exceed 5.7 % of dry mass. To be
 281 sure, the maximal addition in the laboratory probes was set to be 4 % of both waste
 282 coal dust samples. Although the sample CD1 appeared coarser because of
 283 agglomerated grains, the tests showed that CD2 was of somewhat coarser texture
 284 (Table 2). The volumetric method for determining the contents of carbonates showed
 285 that the samples CD did not contain any.

286 The mineralogical analysis (Fig. 4) proved the differences between the BC1
 287 and BC2 samples according to the presence of carbonates. Based on chemical and
 288 mineralogical tests, these samples mostly contained quartz, followed by carbonates
 289 (calcite and dolomite) in BC1, a lower amount of plagioclase-type feldspar and clay
 290 minerals. Iron hydroxides and organic matter were found by DSC/TG analysis (Fig.
 291 5a). It is revealed that the clay minerals in BC1 were mica (L), chlorite (HI), smectite
 292 (Sm), and traces of kaolinite (K), while BC2 was the same except it did not contain K.
 293 Based on XRF, XRD, DSC, and granulometry analysis it is concluded that the higher
 294 quantity of clay minerals was present in the sample BC2.

295



296

297 **Fig. 4.** Mineralogical analysis of the loess clays: (a) BC1 and (b) BC2.

298

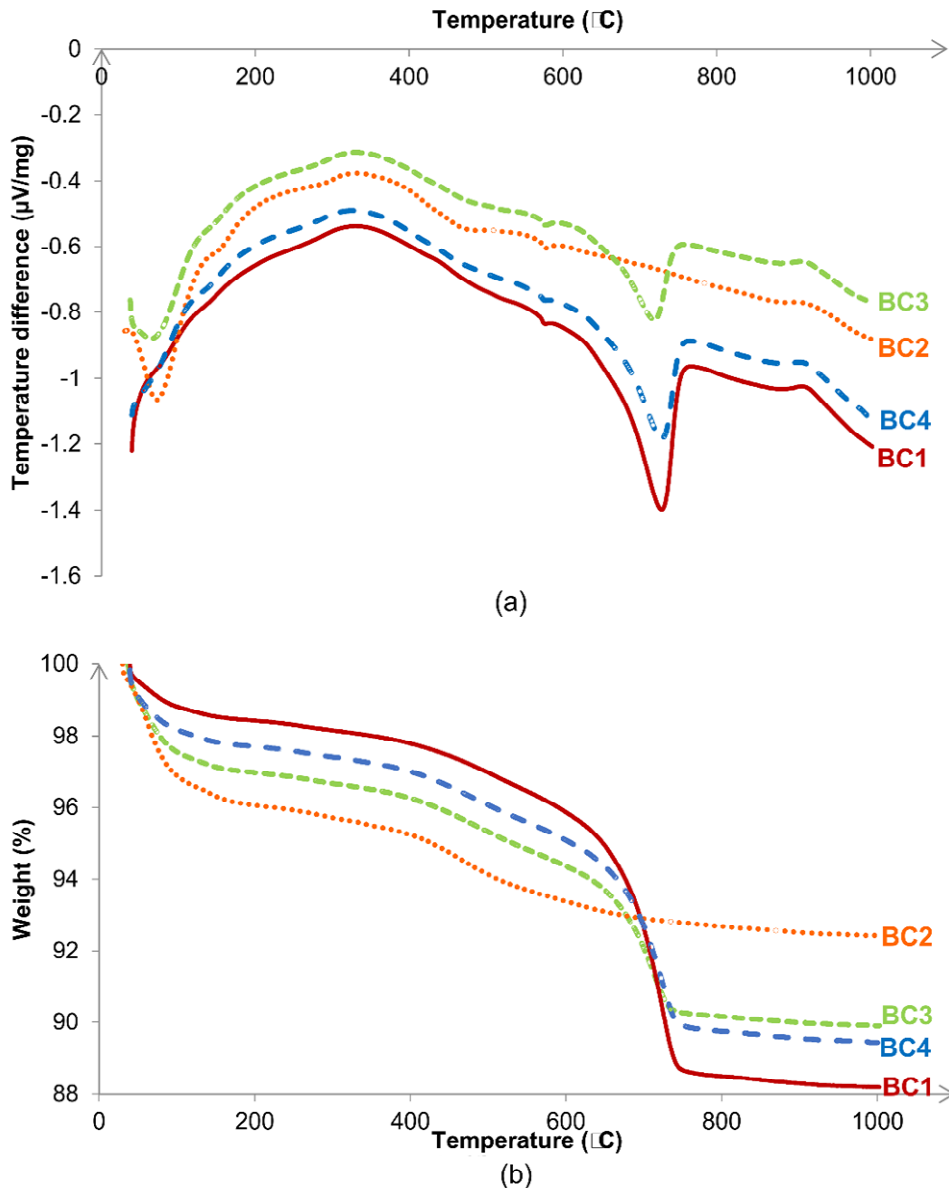
299 From the DSC analyzes presented in Fig. 5a it is seen that the brick clays lose
 300 water with a peak up to a maximum of 74 °C (the loss of adsorbed water). Further, the

301 interlayer water is lost between 100 °C and 200 °C, when BC1 lost 0.39 % and BC2
302 0.81 % of the mass. Judging by the largest mass loss of the BC2 sample in this period,
303 it is expected to have the slightly highest content of clay minerals (Nigay et al., 2017).
304 At about 200 °C the organic matter decomposition begins (Arsenović et al, 2014), with
305 the interruption by small exothermic peaks at about 270 °C -290 °C which
306 corresponded to the transition of goethite to hematite. This reaction was the least
307 pronounced in sample BC1 (Table 1) since the quantity of iron was the lowest
308 (Arsenović et al, 2014). The exothermal maxima of decomposition of organics
309 occurred at 322 °C - 339 °C. The peaks originating from the decomposition of clay
310 minerals are overlapped by burning organic matter. A small peak resulting from quartz
311 transformation is observed in all clays at 574 °C - 578 °C. The decomposition of
312 organic matter took place up to about 600 °C, and the corresponding mass loss was
313 similar in all the brick clays - about 2.6 % (Arsenović et al, 2014). Degradation of
314 carbonates was observed in all the samples except BC2 with endothermic peaks
315 minima at temperatures of 720 °C - 728 °C (Nigay et al., 2017). In the interval 600 °C
316 – 800 °C, sample BC1 lost 7.36 % of the mass, while in the case of BC2 it was about
317 0.7 %. After 800 °C, endothermic reactions occur with small peaks at about 884 °C
318 which could be related to the destruction of the illites` structure (Vasić et al., 2017). At
319 the end of the test, all samples showed a small exothermic peak at 904 °C - 919 °C
320 without the mass loss, which could be related to the formation of spinels, Fe-diopside,
321 and/or amorphous glassy phase, since the mass loss did not occur in that period
322 (Arsenović et al, 2014; Vasić et al., 2017), after which the endothermic processes
323 continued. In the period from 800 °C to 1000 °C, all the clays lost up to 0.3% of the
324 mass.

325 From the DSC analyzes presented in Fig. 6a it is seen that the mixtures with
326 waste coal dust experienced more intensive endothermic peaks than that of brick clays
327 at the beginning of heating since the samples were not completely dry. The greatest
328 loss of mass in the period up to 100 °C (around 3 %) and 200 °C (0.9 %) is noticed in
329 sample C5 (around 3 %), because of high BC1 content. The exothermal process
330 showed max peaks at about 370 °C when the mass loss was also the highest. The
331 curves exhibited small endothermic peaks at about 380 °C, which could be a
332 consequence of organic or maceral impurities from the waste coal dust (Ozbas et al.,
333 2003). The complete organic matter combustion (200 °C – 600 °C) influenced the
334 highest mass loss in C5 (6.1 %), while the lowest was observed in C4 (3.9 %). Sample

335 C2 showed higher content of the released energy than C1, and correspondingly the
336 mass lost in the whole process was slightly higher (C1 – 5.1 %, C2 – 5.6 %). The
337 addition of waste coal dust moved the exothermal maxima towards somewhat higher
338 temperatures, compared to the brick clays alone.

339

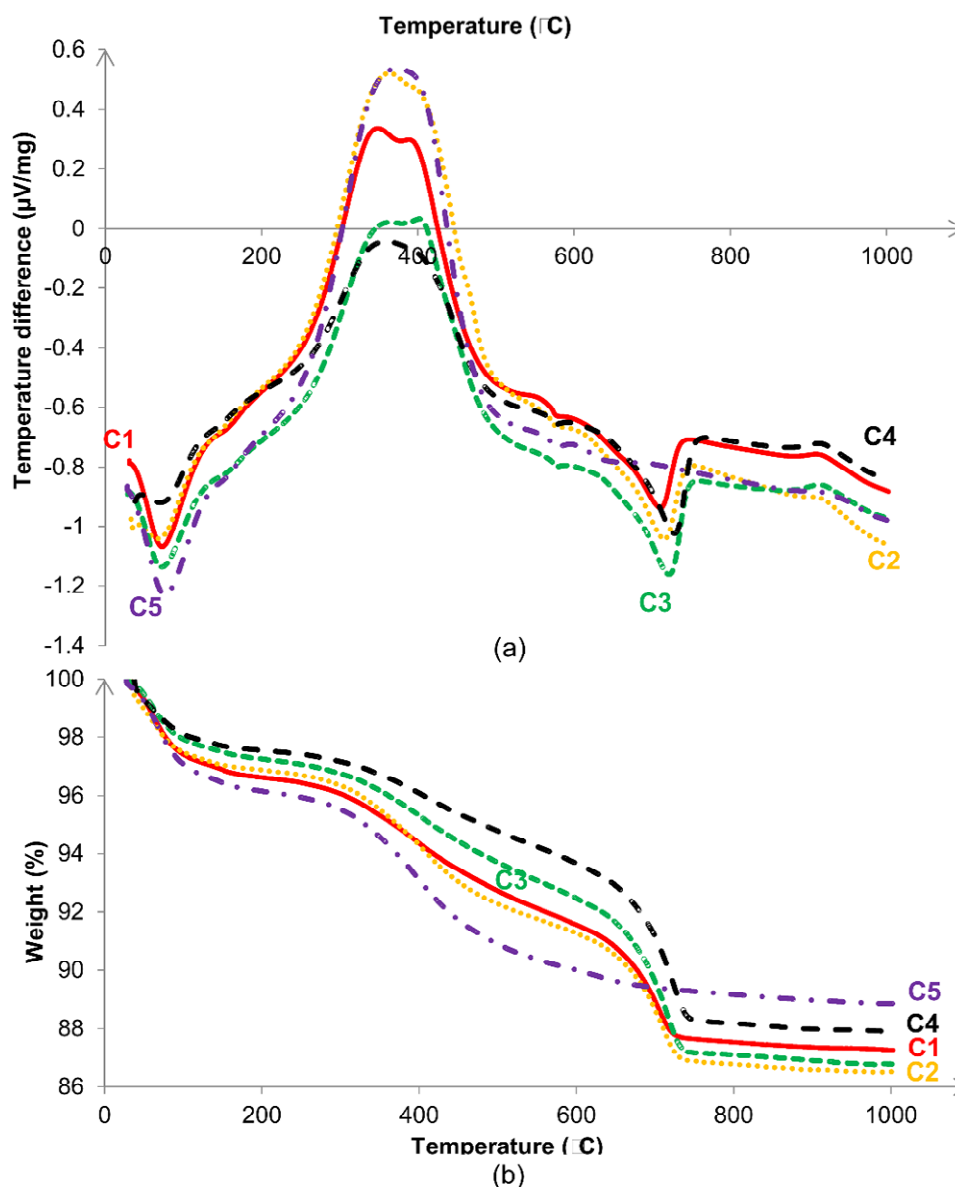


340

341 **Fig. 5.** Simultaneous thermal analyses: (a) DSC of brick clays, and (b) TGA of brick
342 clays.

343

344

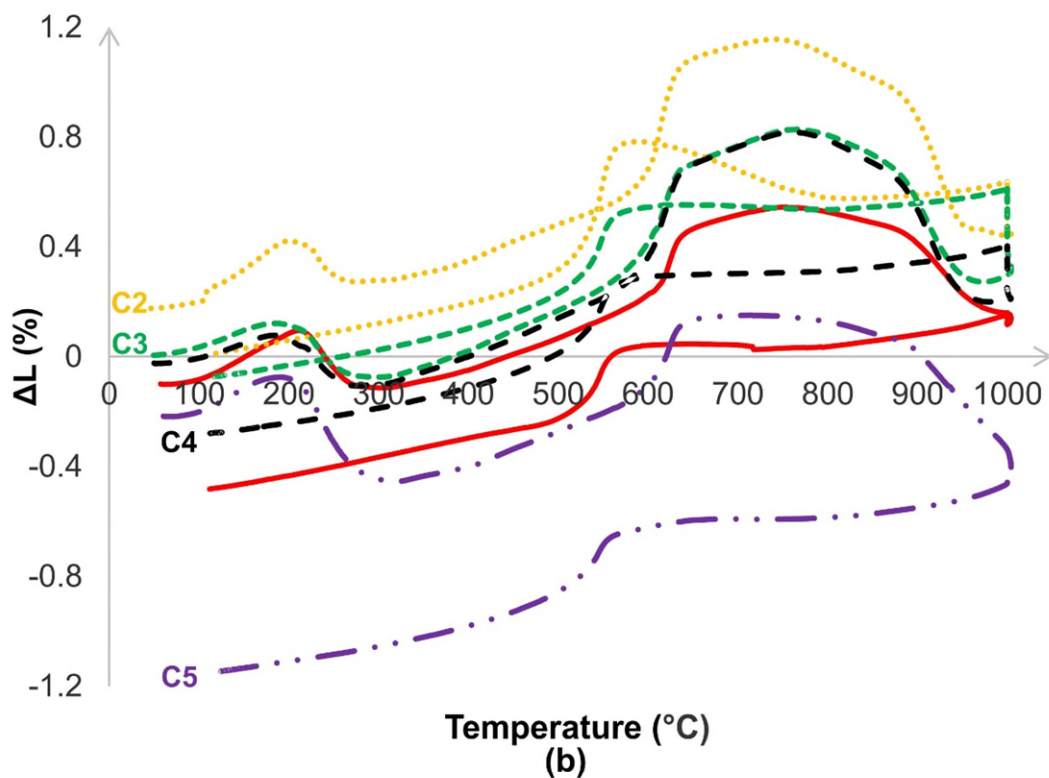
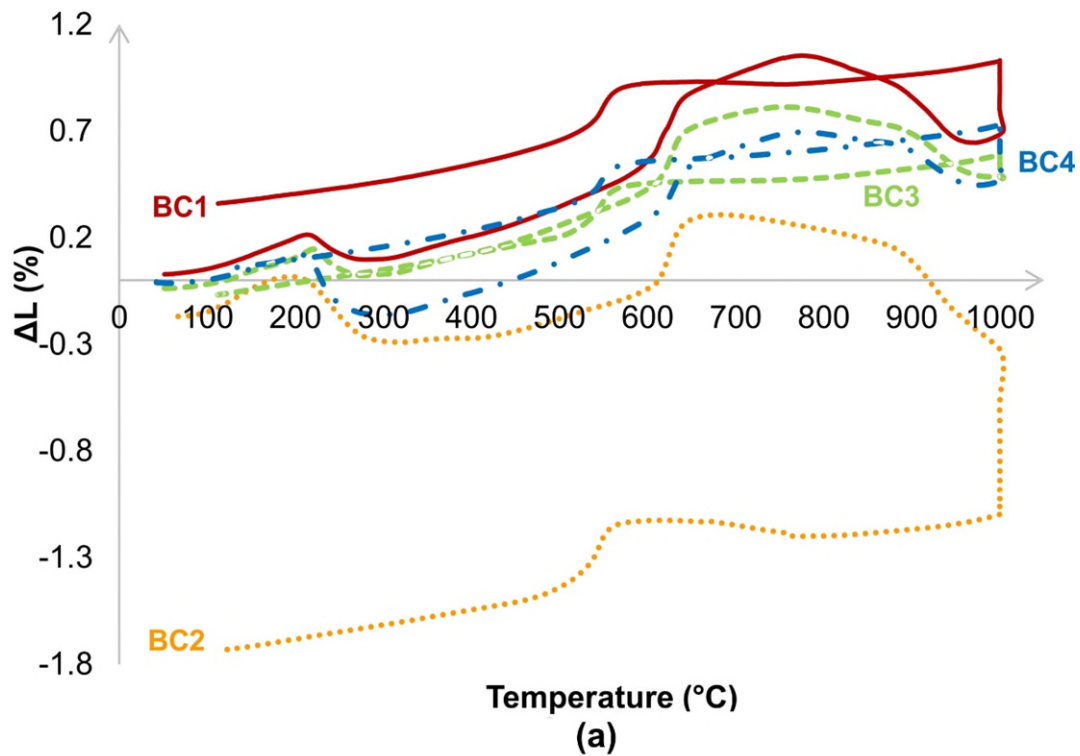


345
 346 **Fig. 6.** Simultaneous thermal analyses: (a) DSC of brick clay-waste coal dust
 347 mixtures and (b) TGA of brick clay-waste coal dust mixtures.

348

349 Dilatometry analyses are presented in Fig. 7. The brick clays (Fig. 7a) showed
 350 similar patterns until about 640 °C. Spreading of up to about 0.2 % until 200 °C – 220
 351 °C, caused by the water removal, is followed by a mild spread until the organic matter
 352 is released (600 °C – 620 °C), and the intensive expansion is noticed up to about 640
 353 °C. This period is followed by a wide peak with the maximum at 890 °C in the samples
 354 BC1, BC3, and BC4, and then an intensive shrinkage due to the decomposition of illite
 355 and the formation of spinel up to 950 °C (up to about 0.4 %). Shrinkage in the
 356 mentioned samples lasted until 980 °C, and then a slight swelling occurred until the

357 final temperature. These then expanded during retention at 1000 °C, and the effect
 358 was the most pronounced in BC1 (about 0.3 %) and least in the case of BC3 (0.1 %).
 359



360
 361 **Fig. 7.** Dilatometric curves of (a) brick clays, (b) clay-waste coal dust mixtures.
 362

363 The expansion that occurred during the retention is rarely reported in the
364 literature (Cobo-Ceacero et al., 2019; Pontikes et al., 2009; Rekecki et al., 2004; Vasić
365 et al., 2017). The expansion is caused and depended mainly on the content of
366 carbonates in the soils that contain relatively low quantities of clay minerals, since high
367 volume anorthite may occur (Vasić et al., 2017). Besides, this effect could be
368 influenced by the content of pure quartz (Mekki et al., 2008). The sample BC2 showed
369 a traditional brick clay dilatometric curve (Vasić et al., 2017), with intensive shrinkage
370 after about 900 °C, and further contraction to about 0.8 % during the retention time.
371 The brick clay samples sintering started around 900 °C, due to the presence of illite.
372 During the cooling period, all the brick clays showed the usual behavior, with a specific
373 peak of quartz` conversion at about 564 °C causing the spreading in the range of 0.2
374 % - 0.3 %.

375 The mixtures of brick clays with waste coal dust represented a similar
376 behavior to BC samples during firing (Fig. 7b). In some cases, the expansion during
377 heating of the samples was moved toward 20 °C - 30 °C lower temperatures range
378 when compared to the pure brick clays (C1 and C2), while in the others, there was no
379 change in the position of the peaks. All the samples, except for C5, experienced
380 spreading while retention at the peak temperature because of the significant presence
381 of carbonates. After the cooling phase, the clay-waste coal dust samples shrank more
382 than the highly calcareous BC4 clay. All the tested combinations showed sintering
383 started after 900 °C, which corresponded to the spinel formation peaks in DSC curves
384 (Fig.5a and Fig.6a).

385

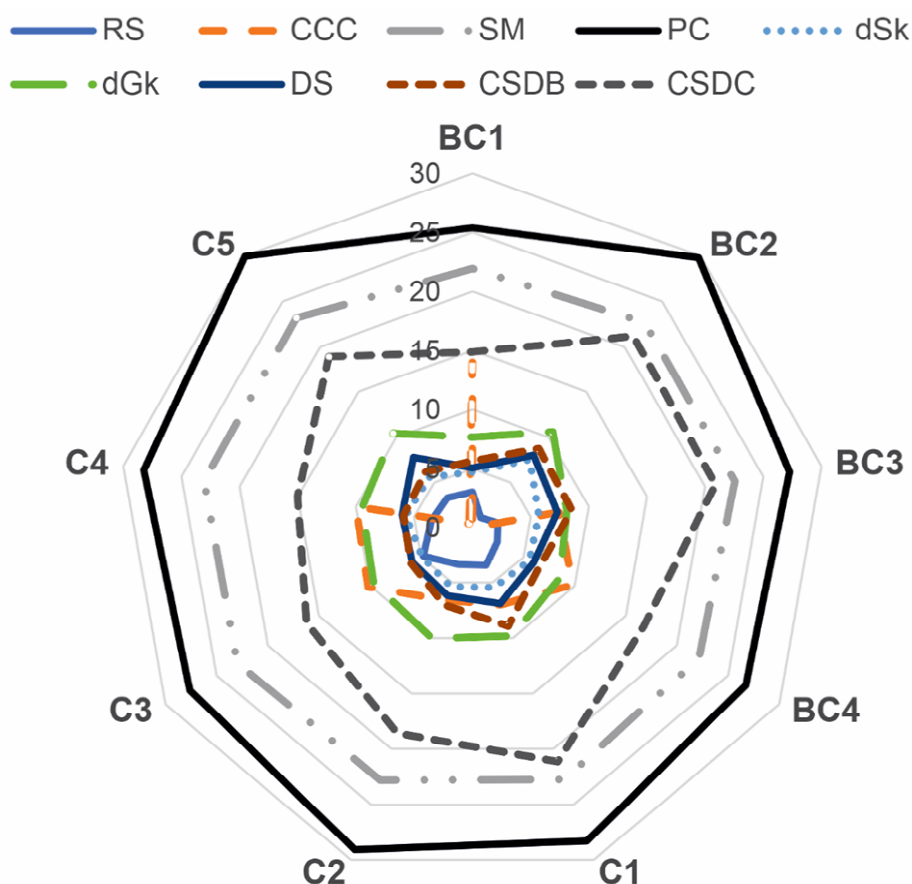
386

387 *3.2. The behavior of the laboratory products during molding and drying*

388

389 After adequate preparation, the raw materials behaved satisfactorily during
390 molding and were classified as materials of good plasticity according to the method by
391 Pfefferkorn (Fig. 8). Among the clays, the sample BC1 showed the lowest plasticity
392 since its` high content of carbonates (Vasić et al., 2017). Most of the materials were
393 susceptible to drying according to Bigot, except for BC2 and C5 which were highly
394 susceptible and the most plastic materials.

395



396
 397 **Fig. 8.** Properties of the laboratory products in shaping and drying (RS – remains on
 398 the 0.063 mm sieve, CCC – total carbonates, SM – shaping moisture, PC –
 399 coefficient of plasticity, dSk – drying shrinkage in a Bigot`s curve critical point, dGk –
 400 mass loss in a Bigot`s curve critical point, DS – drying shrinkage, CSDB –
 401 compressive strength of the dry block, CSDC – compressive strength of the dry
 402 cube).

403
 404 Shrinkage during drying was between about 5 % - 8 %, with the shaping
 405 moisture between 21.9 % - 23.2 %. Remains on the 0.063 mm sieve were low and
 406 varied between 1.1 % - 4.8 %, while CCC was from 0.0 % up to 14.0 %. The
 407 mechanical characteristics of the samples in the dry state were adequate, especially
 408 in the case of cubes without voids. The addition of waste coal dust somewhat
 409 increased shaping moisture, plasticity, sensitivity to drying, and total drying shrinkage.
 410 The results were comparable to the previous results (Arsenović et al., 2015b). The
 411 compressive strength of dry laboratory products was mostly reduced compared to that
 412 of the pure clay bricks, except for C1, when it slightly increased. The highest

413 compressive strength of clay bricks was determined for the BC2, while in dry
 414 composite products that were observed in the case of C1, C2, and C5.

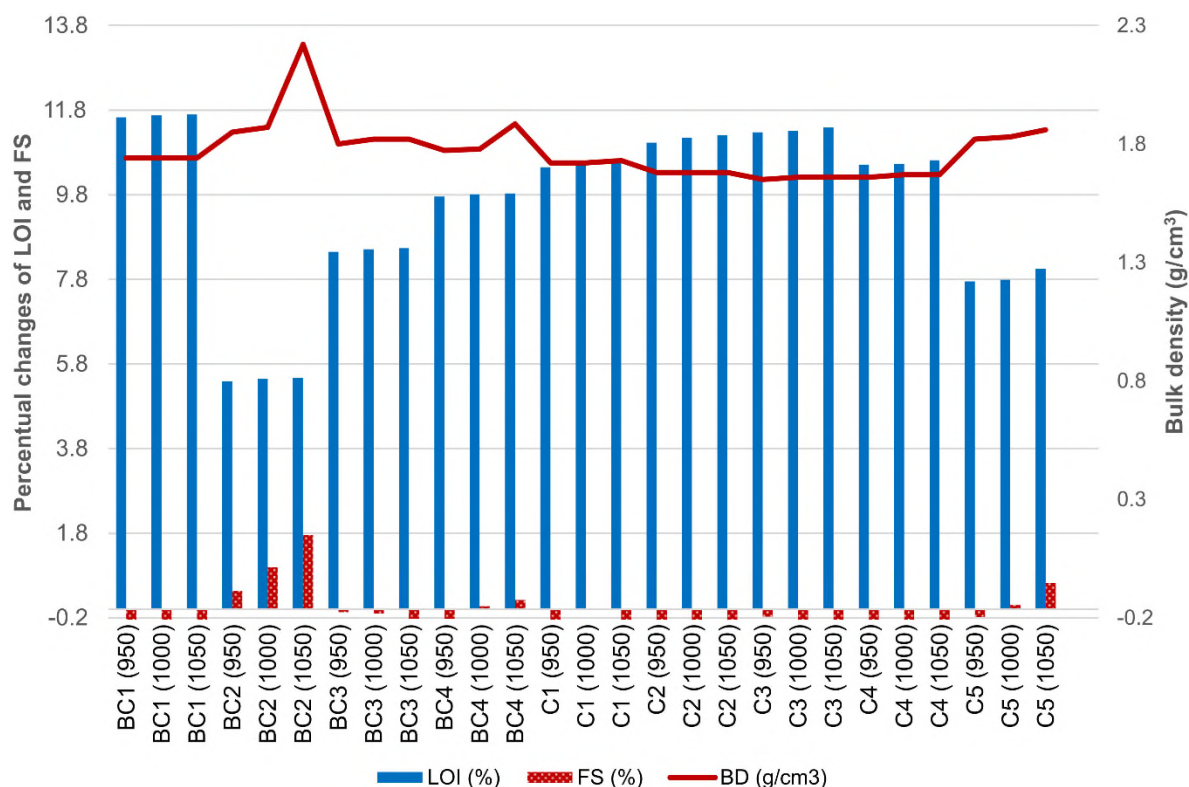
415

416 3.3. Characteristics of the fired laboratory products

417

418 Some of the basic information on the fired products is presented in Fig. 9.

419



420

421 **Fig. 9.** Some characteristics of the products after firing at 950 °C, 1000 °C, and 1050
 422 °C (LOI – loss on ignition, FS – firing shrinkage, BD – bulk density).

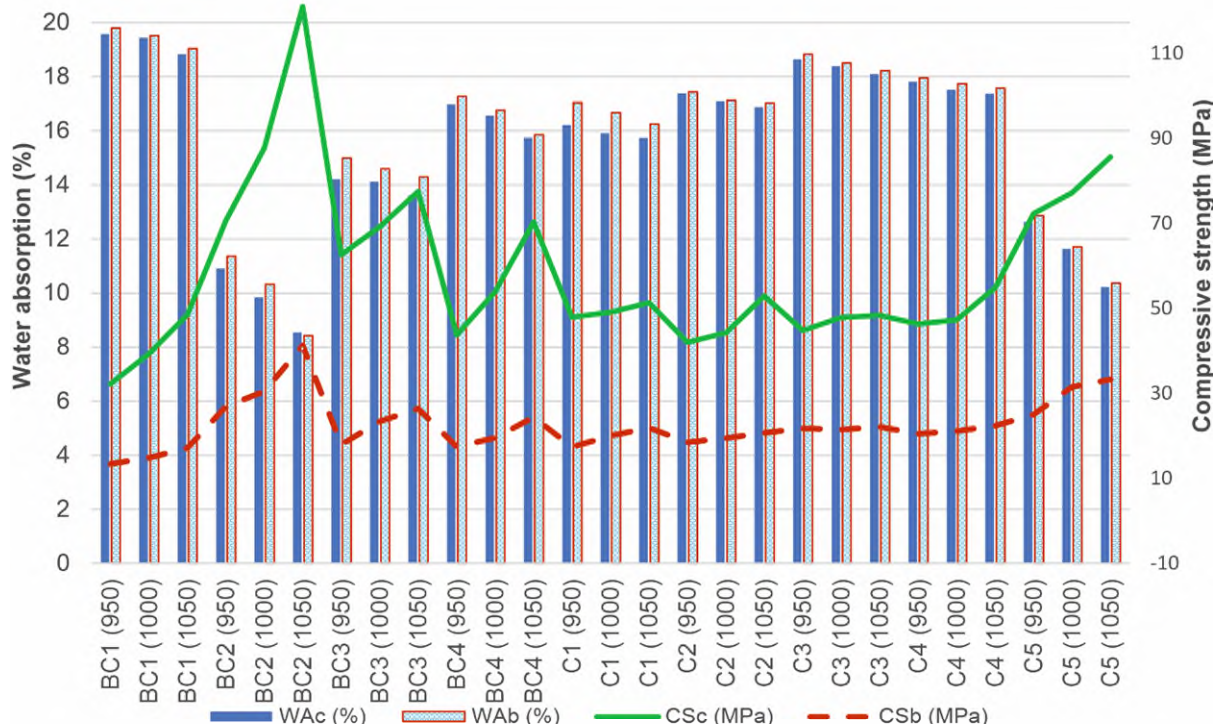
423

424 It is observable that LOI slightly increases with the peak temperature and that
 425 the same is increased with the addition of coal dust. The results match the mass lost
 426 in TGA (Fig. 5b and Fig. 6b). When comparing the LOI values of C3 to C4, and BC2
 427 to C5, it is seen that low changes in the quantity of the added waste coal dust
 428 significantly changed the behavior of samples in the firing. Firing shrinkages showed
 429 that only BC2, BC4, and C5 did not show the expansion while firing at 1000 °C and
 430 1050 °C. The greatest expansion is noticed in the most calcareous BC1 samples,
 431 which was following the dilatometry analyses. The highest bulk density is obtained for
 432 BC2 and BC4 (1050 °C), and the lowest for C3 at 950 °C. The firing temperature

433 influenced BD very moderately. C5 showed the highest BD of all the coal dust-brick
434 clay composites. FS ranged from – 0.56 % - 1.75 % in all the samples. The shrinkage
435 was much lower than the critical 8 % (Weng et al., 2003), but the spreading should be
436 avoided by no retention time at the peak temperature.

437 Laboratory samples fired at 950 °C, 1000 °C, and 1050 °C had a bright red
438 (BC1, BC2, BC3, BC4, C3, and C4) to a brick red color C1, C2, and C5). Weak
439 "popcorns" of lime are noticed in all the samples. Sample BC1 is considered suitable
440 for use in the brick industry for the production of solid bricks. The addition of a more
441 plastic clay with a higher content of clay particles BC2 (Fig.3) to the BC1 sample can
442 enable the production of hollow products and an increase in the mechanical
443 characteristics. By the addition of coal dust, energy-efficient products can be obtained.
444 From the experimental results (Fig. 10) it can be noticed that water absorptions of the
445 cubes (WA_c) and the hollow blocks (WA_b) were similar to each other in all the cases
446 and that the values dropped with the increase in peak temperature. Water absorption
447 in BC1 somewhat decreased with the firing temperature, which is caused by the nature
448 of the raw material and the high content of finely dispersed carbonates. The
449 mechanical characteristics of the hollow products are satisfying and similar to those
450 presented in the literature related to the bricks without voids (Gökçe et al., 2018).
451 There is a slight increase in mechanical characteristics with increasing the peak firing
452 temperature. Compressive strengths differed significantly depending on the structure
453 of the samples: hollow blocks with vertical voids showed about 2 – to 2.5 times lower
454 values. The lowest WAs were found in BC2, while the highest were in the samples
455 BC1 at various firing temperatures, and the situation was vice-versa in terms of the
456 compressive strengths. Among the composites, the highest CSs and the lowest WAs
457 were found in C5, the highest WAs were observed in the C3 samples, while the lowest
458 CSs were determined in C1 and C2. All the samples shown WAs below the critical 20
459 % (Deraman et al., 2018; Muñoz et al., 2019; Özdemir and Sarici, 2020), while the
460 composite brick clay-coal ash bricks showed somewhat lower values of water
461 absorption than previously reported (Gökçe et al., 2018), concerning the lower quantity
462 of the added coal dust. When comparing the results when using coal mines waste
463 containing soil, the results on WA were significantly higher (Özdemir and Sarici, 2020),
464 so as expected energy-efficiency of the newly obtained products.

465



466

467 **Fig. 10.** Water absorption and compressive strength of the laboratory samples fired
 468 at 950 °C, 1000 °C, and 1050 °C (WAc - water absorption of cubes, WAb -water
 469 absorption of hollow blocks, CSc – compressive strength of cubes, CSb –
 470 compressive strength of hollow blocks).

471

472

473

474

475

476

477

478

479

480

481

482

483

484

485

486

The highest mechanical characteristics of all the tested samples were shown by the samples marked C5, given that they contain the highest proportion of clay minerals and low content of carbonates. Since the deposits of loess soils are limited in the amount of more clayey sections, a combination of 70 % BC1 and 30 % BC2 was chosen for the optimal mixture of brick clays. This mixture lowers carbon-footprint when compared to firing BC1 type of clay alone (González et al, 2016). The possible decrease in carbon footprint, when using 97 wt.% of clay consisting of 9.8 % of total carbonates, is estimated to be about 0.3 %, which is a significant amount in industrial conditions. CD1 was chosen as a more suitable additive due to its higher calorific value. Considering the compressive strength and water absorption obtained in sample C3, the chosen amount of CD1 was 3 %. In the case of lower addition of the highly calcareous clay BC1 to the mixture (< 70 %), by using mass containing higher quantities of clay minerals, the increased addition of waste coal dust would be possible (4 % - 4.5 %).

487 **3.4. Firing regime of the industrial-scale products in a tunnel kiln**

488

489 The industrial probe is made based on the composite C3. The hollow blocks
490 with vertical voids of dimensions 250x190x190 mm³ are extruded in the factory. The
491 samples that contained 1.84 % particles above 0.063 mm were of high plasticity,
492 moderate susceptibility to drying while drying shrinkage was 5.74 %. The registered
493 regime, expressed as a function of time, i.e. distance from the entrance to the tunnel
494 kiln, is shown in Fig.11a.

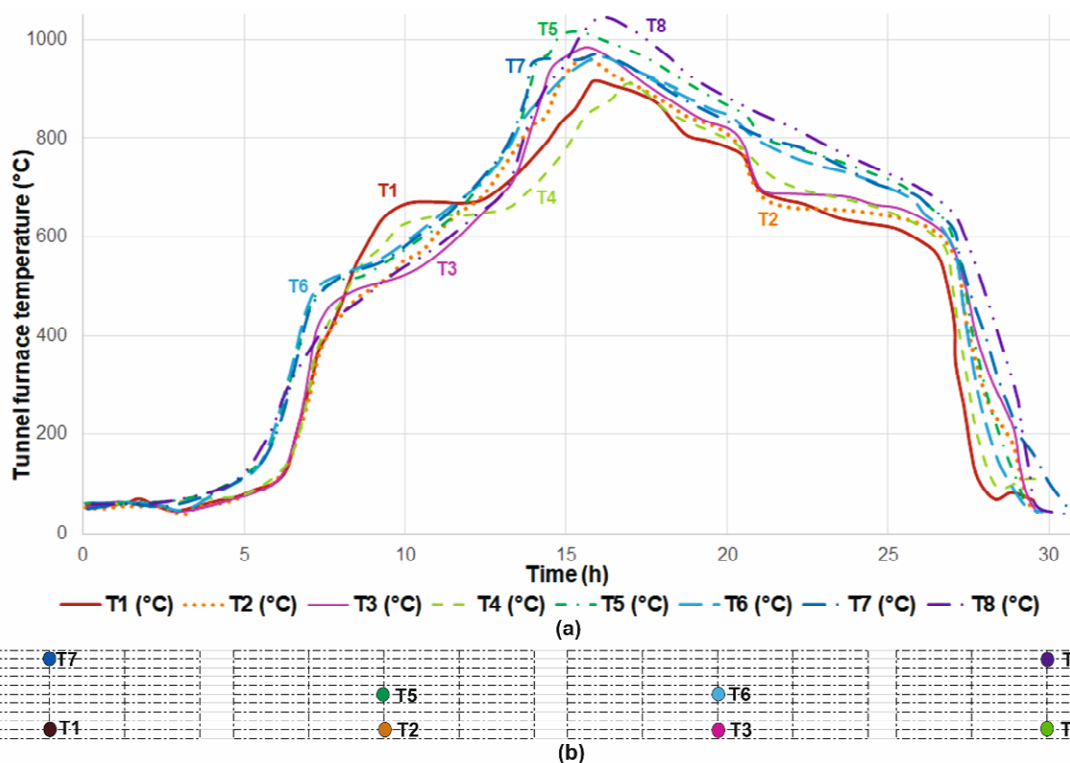


Fig. 11. (a) Firing regime in the tunnel kiln, (b) Position of thermocouples in the wagon (T1 – T8).

495

496

497

498

499

500

501

502

503

504

505

506

507

508

509

510

511

512

513

514

The wagon in the tunnel kiln contained 4x4 stacks with a height of 10 products (190 mm per product). The thrust was such that in 2 h the whole wagon entered the furnace. The frequency of data collection during the recording of the firing regime was 15 minutes for each thermocouple. The locations of the thermocouples during the acquisition of the firing regime were as shown in Fig.11b. Based on the results of the regime's diagnosing (Fig. 11) while subtracting the 2 h in which time the wagon entered the furnace, the duration of the main firing phases is shown in Table 4. It is seen that the lowest peak temperatures are registered at the bottom of the stacks, as expected. The difference between the measured maximum firing temperatures at bottom of the stacks was 140 °C. A difference in temperature (up to 160 °C) in the preheating zone was registered along with the height of the fire channel. It is determined that in some positions of the stack, during both the firing and the cooling zone, the temperature differences were too high (up to 180 °C). The differences in the temperature within the tunnel kiln mean that the quality of products is not uniform. Some of the samples can be lighter in color and not satisfyingly fired, while the others may be over-fired. The lowest peak temperatures were detected in lower positions of the stack due to the air

515 circulating under the wagons and not such a good sealing by using sand (Nicolau and
516 Dadam, 2009).

517

518 **Table 4**

519 Duration of the firing phases and maximum peak temperatures as per thermocouples
520 measurements (T1 – T8).

Thermocouple	Preheating zone (to 750 °C) (h)	Firing zone (750 °C- 1045 °C) (h)	Cooling zone (h)	Total time in the kiln (h)	Maximum peak temperature (°C)
T1	11.93	6.60	9.30	27.83	905
T2	10.83	7.67	9.33	27.83	967
T3	11.43	7.10	9.30	27.83	990
T4	12.27	7.17	8.40	27.83	911
T5	10.63	9.87	7.33	27.83	1016
T6	11.08	9.80	6.95	27.83	964
T7	10.67	9.70	7.47	27.83	967
T8	11.17	10.08	6.58	27.83	1045

521

522 The preheating phase was satisfactorily led, considering the low sensitivity for
523 cracks of loess clays in this period (low drying shrinkage and moderately sensitive
524 nature in drying). The length of the preheating stage was good (approximately 11 - 12
525 hours), as in previous studies (Remmey, 1994; Vasić et al., 2017). The firing phase
526 included significant differences in the peak temperatures and time of retention at
527 different positions, and thus must be corrected. The firing phase lasted up to 10 h but
528 should be prolonged to about 12 h especially because of the addition of the waste coal
529 dust (Vasić et al., 2017). The proposed optimal firing temperature in the tunnel kiln is
530 950 °C. The cooling phase lasted up to 9.3 h and must be prolonged to about 12 h.
531 The phase of slow cooling must be led bearing in mind the phase transformation of
532 quartz (620 °C – 520 °C) when the cooling speed should be of 20 °C/h – 30 °C/h
533 (Nicolau and Dadam, 2009; Vasić et al., 2017). The period of slow cooling in the tunnel
534 kiln has shifted to temperatures higher than 575 °C. The goods in all positions reached

535 575 °C during the period of final intensive cooling when the cooling velocity was 20
536 °C/min – 25 °C/min. The complete firing process should last for about 36 h, which is
537 much shorter than the one needed for other types of clays (Vasić et al., 2017), which
538 makes these clays suitable and economically practical.

539 At the temperatures above 800 °C, products spent between 4.4 h - 8.9 h;
540 above 850 °C, products spent 2.6 h - 7.0 h; and above 900 °C, the products spent 0.0
541 to 3.9 hours in different positions. At positions T1 and T4, products did not even reach
542 900 °C. The temperature of 1000 °C was reached by the products in two positions.
543 The cooling zone is not adapted to the period of phase transformation of quartz when
544 the products are sensitive due to large volume change.

545

546 3.5. Quality of industrial products

547

548 After the extrusion process, 3 moist blocks from the brick kiln were taken and
549 tested in the laboratory. It is determined that drying shrinkage was 0.24 % while firing
550 shrinkage, LOI, and water absorption after firing in the electric furnace were -0.21 %,
551 12.32 %, and 20.33 % respectively. The conditions of drying and firing were as
552 mentioned in *Section 2.3*.

553 After the correction of the firing regime in the tunnel kiln, the products were
554 tested in the laboratory for compressive strength and water absorption determination
555 in different positions of the stack (Table 5). The samples are marked according to the
556 positions of the thermocouples (Fig. 11b).

557 It is seen that the differences in temperatures at the recorded positions in the
558 height of the stack and between the left and right sides of the kiln were still high.
559 Besides, the cooling zone was very unfavorable for the positions T5 and T6 (in the
560 middle) during the quartz transformation phase. For position T1 (bottom left), the
561 quartz transformation phase is at the transition between slow and final rapid cooling.
562 For position S4 (bottom right) the quartz transformation phase is in the middle of
563 slowed cooling. The average compressive strength of the tested blocks is satisfactory
564 and was 11.1 MPa, which was higher than reported earlier in the industrial waste-
565 added products (Munir et al., 2018), though a significant scattering of the results was
566 observed. Low values of the compressive strengths (less than 10 MPa) were obtained
567 for blocks from the middle of the stack were caused by fast cooling in the quartz
568 transformation zone and high heating speed in the heating zone from 300 °C to 600

569 °C. This part of the regime should be slowed down to allow complete combustion of
 570 the organic material before the appearance of the liquid phase in the clay mass. The
 571 compressive strength of the tested blocks from the lower rows was satisfactory (10.2
 572 MPa - 12.5 MPa) comparing to that of relatively low content of clay minerals blocks
 573 (Mylan et al., 2017). The water absorption of these blocks was up to about 18 %.
 574 Despite satisfactory compressive strengths, these products are considered underfired,
 575 since LOI was low (3.7%). The compressive strength of the tested blocks from the
 576 upper rows was satisfactory and amounts to 10.9 MPa to 11.1 MPa. The water
 577 absorption of the blocks fired in the upper rows was about 18 %.

578

579 Table 5

580 Important characteristics of the waste coal dust samples.

	Water absorption (%)	Compressive strength (MPa)	Peak temperature (°C)
Sample T1	18.11	12.5	850
Sample T2	17.68	12.5	805
Sample T3	17.48	11.4	747
Sample T4	17.83	10.2	720
Sample T5	19.21	9.9	920
Sample T6	19.32	9.3	896
Sample T7	19.10	11.1	988
Sample T8	19.15	10.9	953

581

582 4. Conclusions

583

584 This study was the first of a kind examination of the usability of waste coal
 585 dust in fired brick production at several levels. Initially, mixtures of clays and various
 586 samples of waste coal dust were tested at the laboratory level to determine the mineral
 587 and chemical composition, behavior during heating, shaping, drying, and finally,
 588 properties of the products fired between 950 °C and 1050 °C are reported. It is
 589 determined that the low quantities of waste coal dust introduced high changes to the
 590 quality of the laboratory products. It was estimated that the addition of highly caloric
 591 waste coal dust of 3 % is optimal for the given conditions and that by mixing with loess
 592 clay, energy-efficient products are created. The compressive strength of the hollow
 593 laboratory blocks (50 % of voids) made of the optimal mix was around 22 MPa, while
 594 water absorption was between 18.2 % and 18.8 %.

595 The selected mixture was then used to make an industrial probe. The
596 estimated quantity of waste coal dust to be spent daily in the production of 60,000
597 pieces of 250x190x190 mm³ blocks is 12.5 t. In parallel with the assessment of the
598 suitability of the mixture in industry, the firing regime in the tunnel kiln was recorded.
599 It is determined that in some positions of the stack, during both the firing and the
600 cooling zone, the temperature differences were too high (up to 180 °C). The
601 differences in the temperature within the tunnel kiln mean that the quality of products
602 is not uniform. Some of the samples can be lighter in color and not fired enough, while
603 the others may be over-fired. The lowest peak temperatures were detected in lower
604 positions of the stack due to the air circulating under the wagons and not such a good
605 sealing by using sand (Nicolau and Dadam, 2009). After the correction of the regime,
606 the quality of the obtained samples was found to be satisfactory.

607 Further investigations in terms of defining the durability of the obtained
608 products by thaw-freezing tests, then thermal conductivity, and also the determination
609 of leaching of heavy metals are the subjects of the upcoming study.

610

611 **Acknowledgments**

612

613 This study was supported by the Ministry of Education, Science and
614 Technological Development of the Republic of Serbia (Contract No. 451-03-68/2020-
615 14/200012). GG is particularly thankful to the Royal Academy of Engineering, UK to
616 extend financial support via the Indo-UK partnership Industry-academia scheme
617 (Grant No. IAPP18-19\295) with a follow-on funding under the auspices of the
618 Engineering Pandemic preparedness program (EXPP2021\1\277).

619 **References**

620

621 Abi, E., F. Oruç, E. Sabah, 2011. Utilization of waste clay from coal preparation
622 tailings for brick production. *J. Ore Dress.* 13 (25), 22-32.

623 Arsenović, M., Pezo, L., L. Mančić, Radojević, Z., 2014. Thermal and mineralogical
624 characterization of loess heavy clays for potential use in brick industry.
625 *Thermochim. Acta* 580, 38–45. <https://doi.org/10.1016/j.tca.2014.01.026>

626 Arsenović, M., Radojević, Z., Jakšić, Ž., Pezo, L., 2015a. Mathematical approach to
627 application of industrial wastes in clay brick production – Part I: Testing and

- 628 analysis. Ceram. Int. 41(3) 4890 - 4898.
629 <https://doi.org/10.1016/j.ceramint.2014.12.051>
- 630 Arsenović, M., Radojević, Z., Jakšić, Ž., Pezo, L., 2015b. Mathematical approach to
631 application of industrial wastes in clay brick production – Part II: Optimization.
632 Ceram. Int. 41(3), 4899-4905. <https://doi.org/10.1016/j.ceramint.2014.12.050>
- 633 Bocanegra, J.J.C., Mora, E.E., González, G.I.C., 2019. Galvanic sludges:
634 Effectiveness of red clay ceramics in the retention of heavy metals and effects
635 on their technical properties. Environ. Technol. Innov. 16, 100459.
636 <https://doi.org/10.1016/j.eti.2019.100459>
- 637 Chen, X., Zhang, Y., Zhang, Q., Li, C., Zhou, Q., 2015. Thermal analyses of the lignite
638 combustion in oxygen-enriched atmosphere. Therm. Sci. 19 (3), 801 - 811.
639 <https://doi.org/10.2298/TSCI141005007C>
- 640 Cobo-Ceacero, C.J., Cotes-Palomino, M.T., Martínez-García, C., Moreno-Maroto,
641 J.M., Uceda-Rodríguez, M., 2019. Use of marble sludge waste in the
642 manufacture of eco-friendly materials: applying the principles of the Circular
643 Economy. Environ. Sci. Pollut. Res. 26, 35399–35410.
644 <https://doi.org/10.1007/s11356-019-05098-x>
- 645 Deraman, R., Abdullah, A.H.b., Nagapan, S., Abas, N.H., Suratkon, A.B., Hasmori,
646 M.F., 2018. Improving thermal conductivity of fired clay brick using sawdust
647 waste. Asian Journal of Technical Vocational Education And Training
648 (AJTVET) 4 (2018) 1-8.
- 649 Fan, G., Zhang, D., Wang, X., 2014. Reduction and utilization of coal mine waste
650 rock in China: A case study in Tiefa coalfield. Resour. Conserv. Recycl. 83,
651 24– 33. <http://dx.doi.org/10.1016/j.resconrec.2013.12.001>
- 652 Ferrer, S., Mezquita, A., Gomez-Tena, M.P., Machi, C., Monfort, E., 2015. Estimation
653 of the heat of reaction in traditional ceramic compositions. Appl. Clay Sci. 108,
654 28-39. <https://doi.org/10.1016/j.clay.2015.02.019>
- 655 Goel, G., Kalamdhad, A.S., Agrawal, A., 2018. Parameter optimisation for producing
656 fired bricks using organic solid wastes. J. Clean. Prod. 205, 836-844.
657 <https://doi.org/10.1016/j.jclepro.2018.09.116>
- 658 Gökçe, M.V., Akçaözoğlu, S., Sinani, B., 2018. Investigation of production of brick
659 with waste coal powder additive. Proceedings of the 7th annual international
660 conference, International conference on civil engineering, infrastructure and
661 environment, UBT Innovation campus, 26.-28. October 2018, 39-47.

- 662 González, I., Barba-Brioso, C., Campos, P., Romero, A., Galan, E., 2016. Reduction
663 of CO₂ diffuse emissions from the traditional ceramic industry by the addition
664 of Si-Al raw material. *J. Environ. Manage.* 180, 190-196.
665 <http://dx.doi.org/10.1016/j.jenvman.2016.05.039>
- 666 Gupta, N., Gedam, V.V., Moghe, C., Labhasetwar, P., 2017. Investigation of
667 characteristics and leaching behavior of coal fly ash, coal fly ash bricks and
668 clay bricks. *Environ. Technol. Innov.* 7, 152-159.
669 <http://dx.doi.org/10.1016/j.eti.2017.02.002>
- 670 Haibin, L., Zhenling, L., 2010. Recycling utilization patterns of coal mining waste in
671 China. *Resour. Conserv. Recycl.* 54, 1331–1340.
672 <https://doi.org/10.1016/j.resconrec.2010.05.005>
- 673 Kovács, B., Czinkota, I., Tolner, L., Czinkota, G.Y., 2006. FIT method for calculating
674 soil particle size distribution from particle density and settling time data.
675 *Agrokémia és talajtan* 55 (1), 295 – 304.
676 <https://doi.org/10.1556/agrokem.55.2006.1.32>
- 677 Lemeshev, V.G., Gubin, I.K., Savel'ev, Y.A., Tumanov, D.V., Lemeshev, D.O., 2004.
678 Utilization of coal mining waste in the production of building ceramic materials.
679 *Glass Ceram.* 61 (9–10), 308-311. DOI:
680 [10.1023/B:GLAC.0000048698.58664.97](https://doi.org/10.1023/B:GLAC.0000048698.58664.97)
- 681 Li, J., Wang, J., 2019. Comprehensive utilization and environmental risks of coal
682 gangue: A review. *J. Clean. Prod.* 239, 117946.
683 <https://doi.org/10.1016/j.jclepro.2019.117946>
- 684 Lingam, R.K., Suresh, A., Dash, P.S., Sriramoju, S.K., Ra, T., 2016. Upgrading coal
685 washery rejects through caustic-acid leaching. *Min. Proc. Ext. Met. Rev.* 7:2,
686 69-72. <https://doi.org/10.1080/08827508.2015.1115987>
- 687 Mekki, H., Anderson, M., Benzina, M., Ammara, E., 2008. Valorization of olive mill
688 wastewater by its incorporation in building bricks. *J. Hazard. Mater.* 158, 308-
689 315. <https://doi.org/10.1016/j.jhazmat.2008.01.104>
- 690 Munir, M.J., Kazmi, S.M.S., Wu, Y.-F., Hanif, A., Khan, M.U.A., 2018. Thermally
691 efficient fired clay bricks incorporating waste marble sludge: An industrial-
692 scale study. *J. Clean. Prod.* 174, 1122-1135.
693 <https://doi.org/10.1016/j.jclepro.2017.11.060>

- 694 Muñoz, P., Mendivil, M.A., Letelier, V., Morales, M.P., 2019. Thermal and mechanical
695 properties of fired clay bricks made by using grapevine shoots as pore forming
696 agent. Influence of particle size and percentage of replacement. *Constr. Build.*
697 *Mater.* 224, 639-658. <https://doi.org/10.1016/j.conbuildmat.2019.07.066>
- 698 Mylan, R., Maharaj, C., Maharaj, R., 2017. Creating the optimal product formula for
699 use by a heavy clay block manufacturer. *Clay Res.* 35 (2), 71-83.
- 700 Nicolau, V. de P., Dadam, A.P., 2009. Numerical and experimental thermal analysis
701 of a tunnel kiln used in ceramic production. *J. of the Braz. Soc. of Mech. Sci.*
702 & *Eng.* XXXI (4), 297-304. [https://doi.org/10.1590/S1678-](https://doi.org/10.1590/S1678-58782009000400003)
703 [58782009000400003](https://doi.org/10.1590/S1678-58782009000400003)
- 704 Nigay, P.M., Cutard, T., Nzihou, A., 2017. The impact of heat treatment on the
705 microstructure of a clay ceramic and its thermal and mechanical properties,
706 *Ceram. Int.* 43(2), 1747–1754. <https://doi.org/10.1016/j.ceramint.2016.10.084>
- 707 Ozbas, E., Kök, M.V., Hicyilmaz, C., 2003. DSC study of the combustion properties
708 of Turkish coals. *J. Therm. Anal. Calorim.* 71, 849–856.
709 <https://doi.org/10.1023/A:1023378226686>
- 710 Özdemir, E., Sarici, D.E., 2020. Estimation of calorific values of some of the Turkish
711 lignites by Artificial Neural Network and Multiple Regressions. *Curr. Phys.*
712 *Chem.* 10, 1-9. <https://doi.org/10.2174/1877946809666191120125450>
- 713 Pontikes, Y., Rathossi, C., Nikolopoulos, P., Angelopoulos, G.N., Jayaseelan, D.D.,
714 Lee, W.E., 2009. Effect of firing temperature and atmosphere on sintering of
715 ceramics made from Bayer process bauxite residue. *Ceram. Int.* 35, 401–407.
716 <https://doi.org/10.1016/j.ceramint.2007.11.013>
- 717 Rekecki, R., Ranogajec, J., Oszkó, A., Kuzmann, E., 2004. Effects of firing conditions
718 on the properties of calcareous clay roofing tiles. *J. Mater. Civ. Eng.* 26(1),
719 175-183. [https://doi.org/10.1061/\(ASCE\)MT.1943-5533.0000783](https://doi.org/10.1061/(ASCE)MT.1943-5533.0000783)
- 720 Remmey, G.B., 1994. Firing ceramics, *Advanced Series in Ceramics*, Vol. 2, World
721 Scientific.
- 722 Rimpel, E., 2019. Tunnel kiln: Technology overview and project assessment
723 guideline. Remmey, G.B., 1994. Firing ceramics, *Advanced Series in*
724 *Ceramics*, Vol. 2, World Scientific. Available at:
725 [https://www.ccacoalition.org/en/resources/tunnel-kiln-technology-overview-](https://www.ccacoalition.org/en/resources/tunnel-kiln-technology-overview-and-project-assessment-guideline)
726 [and-project-assessment-guideline](https://www.ccacoalition.org/en/resources/tunnel-kiln-technology-overview-and-project-assessment-guideline)

- 727 Soussi, N., Kriaa, W., Mhiri, H., Bournot, P., 2017. Reduction of the energy
728 consumption of a tunnel kiln by optimization of the recovered air mass flow
729 from the cooling zone to the firing zone. *Appl. Therm. Eng.* 124, 1382-1391.
730 <http://dx.doi.org/10.1016/j.applthermaleng.2017.06.111>
- 731 SRPS EN 772-1 Methods of test for masonry units - Part 1: Determination of
732 compressive strength, Institute for standardization of Serbia, Belgrade, 2016.
- 733 SRPS U.B1.018 Testing of soils - Determination of particle size distribution, Institute
734 for standardization of Serbia, Belgrade, 2005.
- 735 SRPS EN 772-13 Methods of test for masonry units - Part 13: Determination of net
736 and gross dry density of masonry units (except for natural stone), Institute for
737 standardization of Serbia, Belgrade, 2010.
- 738 SRPS EN 772-21 Methods of test for masonry units - Part 21: Determination of water
739 absorption of clay and calcium silicate masonry units by cold water absorption,
740 Institute for standardization of Serbia, Belgrade, 2012.
- 741 Stolboushkin, A.Yu., Ivanov, A.I., Fomina, O.A., 2016. Use of coal-mining and
742 processing wastes in production of bricks and fuel for their burning. *Procedia*
743 *Eng.* 150, 1496 – 1502. <https://doi.org/10.1016/j.proeng.2016.07.089>
- 744 Taalab, A.S., Ageeb, G.W., Siam, H.S., Mahmoud, S.A., 2019. Some characteristics
745 of calcareous soils. A review. *Middle East J. Agric. Res.* 8(1), 96-105.
- 746 Taha, Y., Benzaazoua, M., Hakkou, R., Mansori, M., 2016. Coal mine wastes
747 recycling for coal recovery and eco-friendly bricks production. *Miner. Eng.*
748 107, 123-138. <http://dx.doi.org/10.1016/j.mineng.2016.09.001>
- 749 Vasić, M., Pezo, L., Radojević, Z., 2020. Optimization of adobe clay bricks based on
750 the raw material properties (mathematical analysis). *Constr. Build. Mater.* 244,
751 118342. <https://doi.org/10.1016/j.conbuildmat.2020.118342>
- 752 Vasić, M.V., Pezo, L., Zdravković, J.D., Bačkalić, Z., Radojević, Z., 2017. The study
753 of thermal behavior of montmorillonite and hydromica brick clays in predicting
754 tunnel kiln firing curve. *Constr. Build. Mater.* 150, 872-879.
755 <https://doi.org/10.1016/j.conbuildmat.2017.06.068>
- 756 Vasić, M.V., Pezo, L., Zdravković, J.D., Vrebalov, M., Radojević, Z., 2018. Thermal,
757 ceramic and technological properties of clays used in production of roofing
758 tiles – Principal Component Analysis. *Sci. Sinter.* 50 (4), 487-500.
759 <https://doi.org/10.2298/SOS1804487V>

- 760 Vijayan, D.S., Parthiban, D., 2020. Effect of Solid waste based stabilizing material
761 for strengthening of Expansive soil- A review. Environ. Technol. Innov. 20,
762 101108. <https://doi.org/10.1016/j.eti.2020.101108>
- 763 Vukićević, M., Popović, Z., Despotović, J., Lazarević, L., 2018. Fly ash and slag
764 utilization for the Serbian railway substructure transport. Transport 33(2), 389–
765 398. <https://doi.org/10.3846/16484142.2016.1252427>
- 766 Weng, C.H., Lin, D.F., Chiang, P.C., 2003. Utilization of sludge as brick materials,
767 Adv. Environ. Res. 7. 679–685. [http://dx.doi.org/10.1016/S1093-](http://dx.doi.org/10.1016/S1093-0191(02)00037-0)
768 [0191\(02\)00037-0](http://dx.doi.org/10.1016/S1093-0191(02)00037-0)